The Plant Cell, Vol. 19: 2039–2052, June 2007, www.plantcell.org © 2007 American Society of Plant Biologists

Arabidopsis Cytochrome P450 Monooxygenase 71A13 Catalyzes the Conversion of Indole-3-Acetaldoxime in Camalexin Synthesis [W]

Majse Nafisi,[a] Sameer Goregaoker,[b] Christopher J. Botanga,[c] Erich Glawischnig,[d] Carl E. Olsen,[a] Barbara A. Halkier,[a] and Jane Glazebrook[c,1]

[a] Plant Biochemistry Laboratory, Department of Plant Biology, Center for Molecular Plant Physiology, Faculty of Life Sciences, University of Copenhagen, 1871 Frederiksberg C, Denmark

[b] Torrey Mesa Research Institute, San Diego, California 92114

[c] Department of Plant Biology, Center for Microbial and Plant Genomics, University of Minnesota, Saint Paul, Minnesota 55108

[d] Lehrstuhl für Genetik, Technische Universität München, 85350 Freising, Germany

Camalexin (3-thiazol-2-yl-indole) is an indole alkaloid phytoalexin produced by *Arabidopsis thaliana* that is thought to be important for resistance to necrotrophic fungal pathogens, such as *Alternaria brassicicola* and *Botrytis cinerea*. It is produced from Trp, which is converted to indole acetaldoxime (IAOx) by the action of cytochrome P450 monooxygenases CYP79B2 and CYP79B3. The remaining biosynthetic steps are unknown except for the last step, which is conversion of dihydrocamalexic acid to camalexin by CYP71B15 (PAD3). This article reports characterization of CYP71A13. Plants carrying *cyp71A13* mutations produce greatly reduced amounts of camalexin after infection by *Pseudomonas syringae* or *A. brassicicola* and are susceptible to *A. brassicicola*, as are *pad3* and *cyp79B2 cyp79B3* mutants. Expression levels of *CYP71A13* and *PAD3* are coregulated. CYP71A13 expressed in *Escherichia coli* converted IAOx to indole-3-acetonitrile (IAN). Expression of CYP79B2 and CYP71A13 in *Nicotiana benthamiana* resulted in conversion of Trp to IAN. Exogenously supplied IAN restored camalexin production in *cyp71A13* mutant plants. Together, these results lead to the conclusion that CYP71A13 catalyzes the conversion of IAOx to IAN in camalexin synthesis and provide further support for the role of camalexin in resistance to *A. brassicicola*.

INTRODUCTION

Phytoalexins are small antimicrobial compounds produced by plants in response to pathogen attack. A wide variety of different compounds serve as phytoalexins in various plant families. They are thought to contribute to resistance, but in most systems, the evidence for this idea consists solely of antimicrobial activity in vitro. *Arabidopsis thaliana* is thought to produce only a single phytoalexin, camalexin. Very little camalexin is present in healthy *Arabidopsis* plants, but large amounts are produced in response to attack by pathogens, such as *Pseudomonas syringae* bacteria and the necrotrophic fungi *Alternaria brassicicola* and *Botrytis cinerea*. Camalexin synthesis can also be elicited by silver nitrate treatment. Camalexin-deficient mutants have proven useful for elucidating the pathway of camalexin biosynthesis and for testing the role of camalexin in disease resistance in vivo.

Several phytoalexin-deficient (*pad*) mutants that produce reduced amounts of camalexin have been described, but these varied with respect to their effects on susceptibility to pathogens, making it difficult to draw conclusions about the role of camalexin in disease resistance (Glazebrook and Ausubel, 1994; Glazebrook et al., 1997). Three of the *PAD* genes have been identified by map-based cloning. *PAD4* encodes a regulator that affects expression of many pathogen-inducible genes, making *pad4* mutants unsuitable for studies of the role of camalexin in disease resistance (Jirage et al., 1999; Glazebrook et al., 2003). *PAD2* encodes γ-glutamyl cysteine synthase, an enzyme required for synthesis of glutathione (Parisy et al., 2007). The role of glutathione in camalexin synthesis or other aspects of plant defense is not clear, but it seems likely that the reduced glutathione levels in *pad2* mutants could affect multiple aspects of plant metabolism. *PAD3* encodes the cytochrome P450 monooxygenase CYP71B15. This observation, together with the fact that *PAD3* is strongly induced by *P. syringae*, led to the idea that *PAD3* encodes an enzyme required for camalexin biosynthesis (Zhou et al., 1999). This idea was confirmed by the demonstration that PAD3 catalyzes the oxidative decarboxylation of dihydrocamalexic acid to camalexin (Schuhegger et al., 2006).

The *pad3-1* allele is null, and there is almost no camalexin in *pad3-1* plants, making them useful for testing the contribution of camalexin to resistance against various pathogens (Zhou et al., 1999). Camalexin does not contribute substantially to resistance to the biotrophic oomycete *Hyaloperonsopsora parasitica* (Glazebrook et al., 1997), the biotrophic ascomycete *Erysiphe orontii* (Reuber et al., 1998), or the hemibiotrophic bacterium *P. syringae* (Glazebrook and Ausubel, 1994). By contrast, the enhanced

[1] To whom correspondence should be addressed. E-mail jglazebr@umn.edu; fax 612-624-6264.

The author responsible for distribution of materials integral to the findings presented in this article in accordance with the policy described in the Instructions for Authors (www.plantcell.org) is: Jane Glazebrook (jglazebr@umn.edu).

[W] Online version contains Web-only data.

www.plantcell.org/cgi/doi/10.1105/tpc.107.051383

susceptibility of *pad3* mutants to the necrotrophic ascomycetes *A. brassicicola* (Thomma et al., 1999), *B. cinerea* (Ferrari et al., 2003), and *Leptosphaeria maculans* (Bohman et al., 2004) suggests that camalexin limits the growth of these pathogens.

Induction of many plant defense responses depends on signaling mediated by oxylipins, such as jasmonic acid, ethylene, or salicylic acid (SA). Control of camalexin synthesis appears to be largely independent of these signals. Mutations in *coi1* (which block oxylipin signaling) or in *sid2* or *npr1* (which block SA synthesis and SA responses, respectively) have no effect on pathogen-induced camalexin production (Glazebrook et al., 1996; Nawrath and Metraux, 1999; van Wees et al., 2003). Ethylene signaling may play a role, as *ein2* mutants accumulate reduced amounts of camalexin after *P. syringae* infection, but *ein2* does not compromise *A. brassicicola*–induced camalexin synthesis (Heck et al., 2003; van Wees et al., 2003). Camalexin production in response to infection by virulent *P. syringae* strains requires *PAD4*, but *PAD4* is not required for camalexin production induced by *A. brassicicola* or avirulent *P. syringae* strains (Zhou et al., 1998; van Wees et al., 2003).

Recent work has defined some of the enzymatic steps in camalexin synthesis. The cytochrome P450 enzymes CYP79B2 and CYP79B3, which catalyze the conversion of Trp to indole-3-acetaldoxime (IAOx) (Hull et al., 2000; Mikkelsen et al., 2000), are required for camalexin biosynthesis (Glawischnig et al., 2004). This was demonstrated genetically by the complete lack of camalexin in a *cyp79B2 cyp79B3* background (Glawischnig et al., 2004). IAOx is thus a key metabolic branch point, as it is also a precursor for indole glucosinolate and auxin biosynthesis (Bak et al., 2001; Hansen et al., 2001; Zhao et al., 2002). In the biosynthesis of indole glucosinolates, IAOx is oxidized to the corresponding *aci*-nitro or nitrile oxide compound by CYP83B1 (Bak et al., 2001; Hansen et al., 2001). Mutants with defects in *CYP83B1* accumulate elevated levels of free indole-3-acetic acid (IAA) and have high-auxin phenotypes (Delarue et al., 1998; Barlier et al., 2000; Bak et al., 2001). The route from IAOx to auxin is not known, but it is speculated that indole-3-acetonitrile (IAN) and/or indole-3-acetaldehyde may be involved (Pollmann et al., 2006). No IAOx-metabolizing enzymes in the camalexin biosynthetic pathway have been described. The thiazole ring of camalexin was proposed to be derived from Cys based on incorporation of labeled Cys, but not Met, into camalexin (Zook and Hammerschmidt, 1997). It was proposed that Cys condenses with indole-3-carboxaldehyde to form a product that subsequently cyclizes to form the thiazole ring (Browne et al., 1991). The last step of camalexin biosynthesis is conversion of dihydrocamalexic acid to camalexin, which is catalyzed by CYP71B15 (PAD3) (Schuhegger et al., 2006).

In this article, we demonstrate the involvement of the CYP71A13 enzyme in camalexin biosynthesis and pathogen resistance. We describe genetic and biochemical characterization of the CYP71A13 enzyme and show that mutations in the *CYP71A13* gene result in camalexin deficiency and enhanced susceptibility to *A. brassicicola*. When expressed in two heterologous systems, CYP71A13 catalyzed the dehydration of IAOx to IAN, which is the first committed step in the biosynthesis of camalexin. Application of exogenous IAN restored camalexin synthesis in *cyp71A13* knockout mutants.

RESULTS

CYP71A13 Is Required for Resistance to *A. brassicicola*

In a previous expression profiling experiment, many *Arabidopsis* genes were found to be induced in response to infection by *A. brassicicola* (van Wees et al., 2003). To identify genes that contribute to resistance to this pathogen, we isolated mutants homozygous for T-DNA insertions in these genes and tested them for susceptibility to *A. brassicicola*. One of the genes studied was At2g30770, which encodes cytochrome P450 monooxygenase 71A13.

We analyzed two T-DNA insertion alleles of *cyp71A13*, SALK 105136 (*cyp71A13-1*) and SAIL 505 E09 (*cyp71A13-2*) (Sessions et al., 2002; Alonso et al., 2003). Plants homozygous for each insertion were identified using a PCR test. The mutant plants did not show any obvious morphological phenotypes. The positions of the insertions were verified by DNA sequencing of PCR products spanning the junctions of the left borders of the T-DNAs and the genome. Figure 1 shows that the insertions in *cyp71A13-1* and *cyp71A13-2* lie in the third and first exons, respectively. Both insertions are upstream from the Prosite heme-iron ligand signature (amino acids 432 to 441). This heme binding domain is essential for the functions of cytochrome P450 monooxygenases (Schuler and Werck-Reichhart, 2003). Consequently, both insertion alleles are likely to be null mutations.

Both *cyp71A13* mutants were tested for susceptibility to *A. brassicicola*. Droplets (10 μL) containing10^5 spores/mL were placed on the third, fourth, and fifth true leaves of each plant. Disease was assessed 3 d later. As shown in Figure 2, resistant wild-type plants developed necrotic spots at the sites of the inoculation droplets, while both *cyp71A13* mutants developed spreading necrotic lesions similar to those on *pad3-1* plants. At least 20 infected leaves of each genotype were assigned to one of four disease severity classes, as shown in Figure 3. Clearly, both *cyp71A13* mutants are much more susceptible to *A. brassicicola* than wild-type plants.

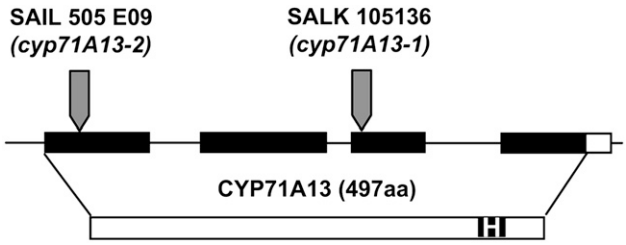

Figure 1. Positions of T-DNA Insertions in At2g30770.

The gene model from The Arabidopsis Information Resource (www.arabidopsis.org) is shown. Exons are represented by rectangles and introns and untranscribed regions by lines. Black fill indicates translated sequences. The protein sequence is represented by the bottom rectangle. The filled region labeled "H" represents the heme-iron ligand signature. Positions of the T-DNA insertions are indicated by arrows. aa, amino acids.

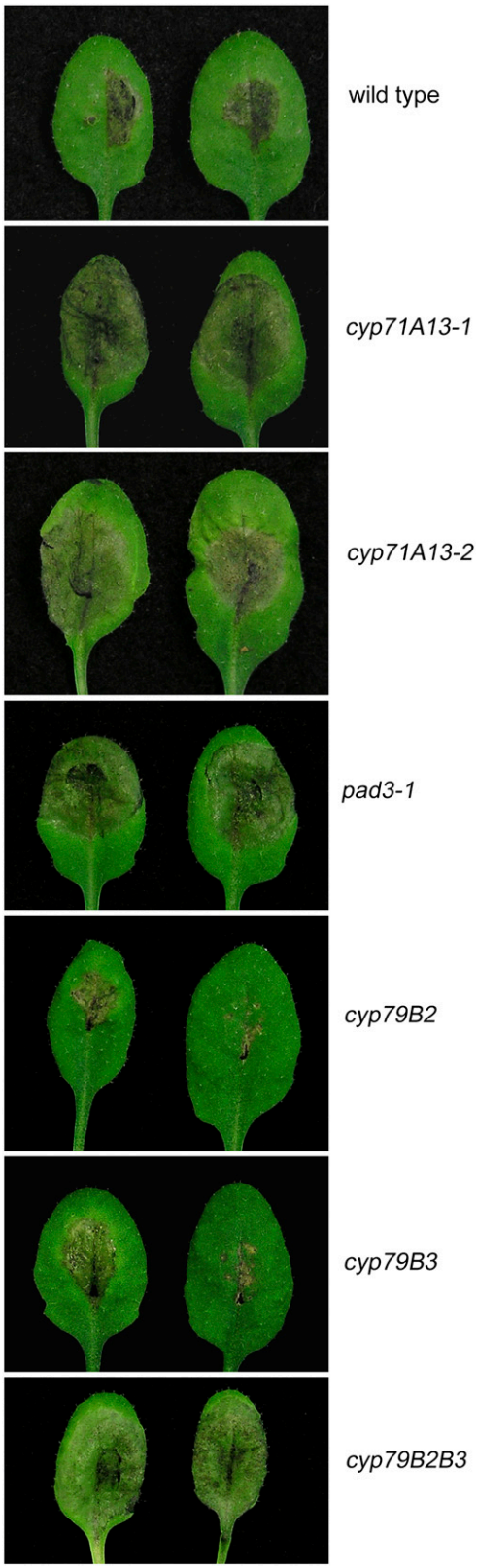

Figure 2. Susceptibility of Various *Arabidopsis* Mutants to *A. brassicicola*.

Leaves 3 d after inoculation. Plants were 24 d old when they were inoculated with *A. brassicicola*. The fifth true leaves from two plants of each genotype are shown.

CYP71A13 Is Required for Camalexin Production

The fact that camalexin-deficient *pad3-1* plants are susceptible to *A. brassicicola* led us to suspect that the *A. brassicicola*–susceptible *cyp71A13* mutants might also be camalexin deficient. We first used *A. brassicicola* infection to induce camalexin accumulation. After 3 d, entire infected leaves were excised, and camalexin levels were determined. Figure 4A shows that camalexin levels in infected *cyp71A13* mutants were <20% of wild-type levels, even though the ratio of infected to uninfected leaf area was much larger in the mutants than in the wild type. Camalexin was not detected in *pad3-1* plants. We next used *P. syringae* infection to induce camalexin accumulation and assayed camalexin 2 d later. Again, camalexin levels in both *cyp71A13* mutants were much lower than in wild-type plants, and no camalexin was detected in *pad3-1* plants (Figure 4B). Camalexin was not detected in uninfected plants of any genotype (data not shown).

Plants carrying T-DNA insertion mutations may carry unknown second-site mutations that are the real causes of observed phenotypes attributed to T-DNA insertions in genes of interest. It is unlikely that the *A. brassicicola*–susceptible and camalexin-deficient phenotypes that we observed in the *cyp71A13* mutants are due to second-site mutations because we observed these phenotypes in plants containing two independent mutant alleles. We conclude that CYP71A13 is required for wild-type levels of camalexin synthesis and *A. brassicicola* resistance in *Arabidopsis*. It is likely that the camalexin deficiency causes the *A. brassicicola* susceptibility because *pad3-1* plants, which cannot perform the last step of camalexin synthesis, are also susceptible to *A. brassicicola*.

Camalexin synthesis is not completely abolished in *cyp71A13* mutants, so there is likely another enzyme that can perform the same function. A reasonable candidate is CYP71A12 (At2g30750) because it is the *Arabidopsis* CYP450 most closely related to CYP71A13 (89% identical amino acids). We obtained a line homozygous for a T-DNA insertion in this gene (GABI-Kat 127 H03; Rosso et al., 2003). When camalexin was determined 2 d after infection with *P. syringae*, no reduction in camalexin levels relative to wild-type plants was observed (see Supplemental Figure 1 online). It remains possible that CYP71A12 and CYP71A13 have similar activities, but that the contribution of CYP71A12 to camalexin synthesis is small relative to that of CYP71A13, and so no diminution of camalexin levels can be observed in *cyp71A12* mutants when CYP71A13 is present. Construction of a double mutant is impractical because the two genes are closely linked. We cannot exclude the possibility that another enzyme is responsible for the residual camalexin in *cyp71A13* mutants.

CYP79B2 and CYP79B3 Are Required for *A. brassicicola* Resistance and Pathogen-Induced Camalexin Production

CYP79B2 and CYP79B3 convert Trp to IAOx (Hull et al., 2000; Mikkelsen et al., 2000), which is known to be a precursor to camalexin because a *cyp79B2 cyp79B3* double mutant does not

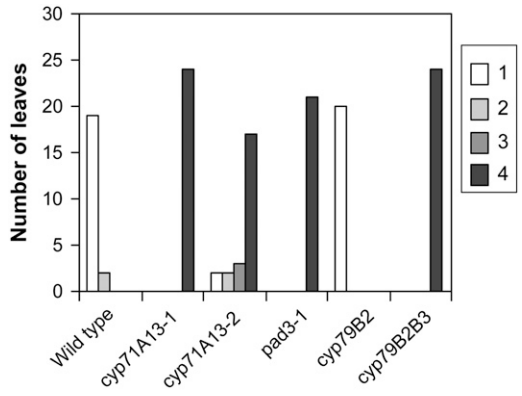

Figure 3. Disease Index Scoring of *A. brassicicola*–Infected Plants.

Plants (21 d old) were inoculated as above. After 3 d, 20 to 24 leaves per genotype were assigned a disease index score. 1, necrosis confined to the area of the inoculation droplet; 2, some chlorosis around the necrotic spot; 3, spreading chlorosis and/or some necrosis beyond the inoculation droplet; 4, spreading necrosis.

produce camalexin after silver nitrate treatment (Glawischnig et al., 2004). We studied the roles of these enzymes in camalexin production and disease resistance during interactions with *P. syringae* and *A. brassicicola*. Following *P. syringae* infection, camalexin levels in *cyp79B2* were approximately half of wild-type levels, *cyp79B3* was indistinguishable from the wild type, and camalexin was undetectable in *cyp79B2 cyp79B3* double mutants (Figure 4B). Similar results for *cyp79B2* and *cyp79B2 cyp79B3* were observed following *A. brassicicola* infection (Figure 4A). These results agree with those obtained by Glawischnig et al. (2004) following elicitation with silver nitrate and Kliebenstein et al. (2005) following infection with *B. cinerea*.

The *cyp79B2 cyp79B3* double mutant was as susceptible to *A. brassicicola* as *pad3-1* and *cyp71A13* mutants (Figures 2 and 3). This observation strengthens the conclusion of Thomma et al. (1999) that the *A. brassicicola* susceptibility of *pad3-1* indicates that camalexin plays a critical role in *A. brassicicola* resistance. Taken together with these previous results, all of four mutants with severe reductions in camalexin levels are susceptible to *A. brassicicola*. Susceptibility to *A. brassicicola* was not observed in *cyp79B2* or *cyp79B3* single mutants (Figures 2 and 3; data not shown). Apparently, the modest reduction in camalexin in *cyp79B2* plants does not compromise resistance to *A. brassicicola*.

Camalexin Deficiency Does Not Compromise Resistance to *P. syringae*

While camalexin-deficient *pad4* and *pad2* plants display enhanced susceptibility to *P. syringae*, *pad3* plants do not. These observations led to the conclusion that camalexin itself does not play a major role in limiting *P. syringae* growth and that enhanced susceptibility of *pad2* and *pad4* plants likely results from pleiotropic effects on other defense responses. To test this idea further, the susceptibility of *cyp71A13* and *cyp79B* mutants to *P. syringae* was examined (see Supplemental Figure 2 online). While *pad4* plants displayed characteristic extreme susceptibility to this pathogen, no increase in pathogen growth relative to wild-type plants was observed in either *cyp71A13* mutant, *cyp79B2*, *cyp79B3*, or the *cyp79B2 cyp79B3* double mutant. This is consistent with the idea that camalexin does not play a major role in resistance to *P. syringae*. The *cyp79B2 cyp79B3* double mutant also fails to produce indole glucosinolates, so

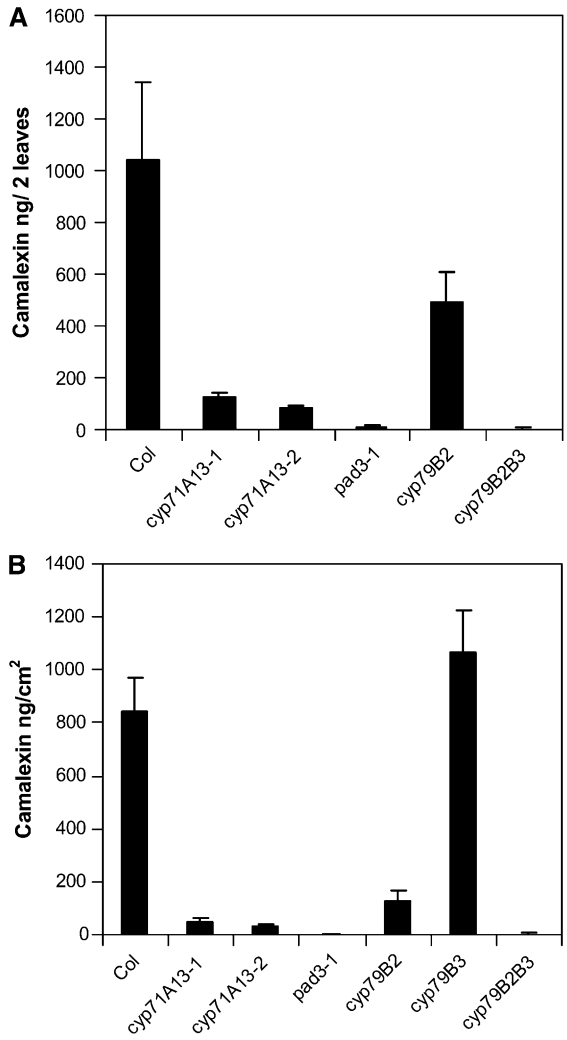

Figure 4. Camalexin Levels in Various *Arabidopsis* Mutants after Infection by Pathogens.

(A) Infection by *A. brassicicola*. Plants were inoculated with *A. brassicicola* spores as described in Methods. After 3 d, entire leaves were excised and camalexin was determined. Each sample consisted of two leaves, and each bar represents the mean and SD of eight replicate samples. Col, Columbia.

(B) Infection by *P. syringae*. Plants were inoculated with bacteria at a starting density of 4×10^4 colony-forming units/cm^2 ($OD_{600} = 0.004$). After 48 h, samples consisting of 1 cm^2 of leaf were excised using a cork borer, and camalexin was determined. Bars represent the means and SD of eight replicates. No camalexin was observed in uninfected leaves of any genotype (data not shown).

these compounds must not play major roles in limiting *P. syringae* growth.

PAD3 and *CYP71A13* Are Coregulated

PAD3 is rapidly induced in response to *P. syringae* infection (Zhou et al., 1999). To determine whether this is true of other genes involved in camalexin synthesis, the expression levels of *PAD3*, *CYP71A13*, *CYP71A12*, *CYP79B2*, and *CYP79B3* were examined in expression profiling data of wild-type plants infected with *Psm* ES4326 obtained using the ATH1 GeneChip array from Affymetrix. Figure 5A shows that *PAD3*, *CYP71A13*, and *CYP79B2* were all strongly induced by 9 h after infection, and their expression levels increased further over the course of the experiment. *CYP79B3* was not induced by infection. Expression of *CYP71A12* was induced by infection, although its induced level appeared to be substantially lower than *PAD3*, *CYP71A13*, and *CYP79B2* (note that gene-to-gene comparisons are unreliable due to variations in the hybridization efficiency of different oligonucleotides on the array).

The Genevestigator database of *Arabidopsis* expression profiling data was used to test for coregulation among pairs of these five genes (Zimmermann et al., 2004). Arrays in which expression of both *PAD3* and *CYP71A13* was significantly above background ($P < 0.05$) were selected from the 1432 ATH1 arrays in the database. Then, for each of the resulting 459 arrays, the $\log_2$ expression values for each gene were plotted as shown in Figure 5B. The correlation between the expression levels of these two genes was quite strong ($r^2 = 0.72$ by linear regression). This coregulation was much weaker in the case of *CYP79B2*. The r^2 values for *CYP79B2* versus *PAD3* and *CYP79B2* versus *CYP71A13* were 0.20 and 0.27, respectively. The P values for all comparisons were smaller than the lower limit for calculation in R, $P < 2.2 \times 10^{-16}$, indicating that all the r^2 values were significantly different from 0. While high expression levels of *PAD3* and *CYP71A13* were associated with high expression levels of *CYP79B2*, there were many arrays in which expression of *CYP79B2* was high but *PAD3* and *CYP71A13* were not. This likely reflects the role of *CYP79B2* in biosynthesis of other compounds in addition to camalexin.

To further investigate coregulation of *PAD3* and *CYP71A13*, we used quantitative RT-PCR (qRT-PCR) to monitor expression of these genes over the course of infection in plants with defense signaling mutations and in wild-type plants. We included *dde2*, in which jasmonic acid signaling is blocked due to a mutation in allene oxide synthase; *ein2*, in which ethylene signaling is blocked; *pad4*, in which SA signaling and expression of many other pathogen-responsive genes is reduced; and *sid2*, in which SA synthesis is greatly reduced. Levels of *PAD3*, *CYP71A13*, and *CYP79B2* mRNAs were determined immediately after infection with *Psm* ES4326 and 6, 9, and 24 h later. The data are provided as Supplemental Table 2 online and summarized in Table 1. The expression patterns of *PAD3* and *CYP71A13* were very similar. Both genes were strongly induced in wild-type plants (see Supplemental Table 2 online) and expressed at lower levels in *pad2*, *pad4*, and *sid2* mutants at 6 and 9 h after infection, in *ein2* mutants at 9 h after infection, and at levels higher than wild-type in *sid2* plants 24 h after infection. By contrast, none of the regulatory mutations affected *CYP79B2* expression except *pad4*, where the effect was only evident at 9 h after infection. These results extend the conclusion that *PAD3* and *CYP71A13* are tightly coregulated, while *CYP79B2* is not.

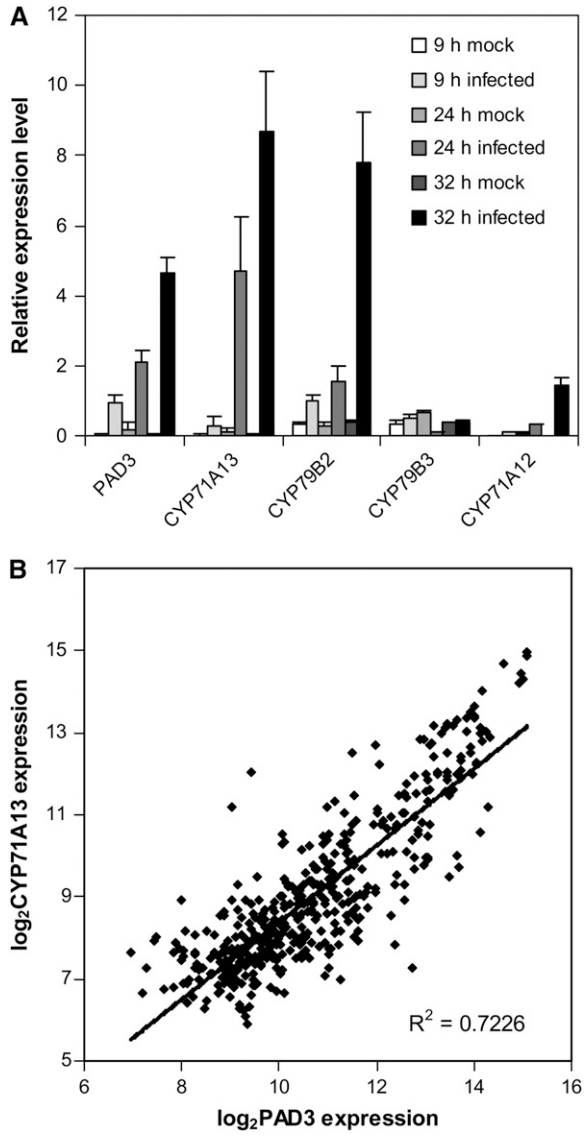

Figure 5. Expression Patterns of Selected Genes during *P. syringae* Infection as Measured by Microarray Experiments.

(A) Expression changes in response to infection by *Psm* ES4326. Expression values were determined using robust multichip average and divided by 1000 for convenience. Each bar represents the mean and SD of three independent replicates.

(B) Comparison of *PAD3* and *CYP71A13* expression patterns. Data points represent $\log_2$-transformed values from the Genevestigator database. The underlying data are provided as Supplemental Table 1 online.

Recombinant CYP71A13 Metabolizes IAOx to IAN

The camalexin-deficient phenotype of *cyp71A13* mutants and the correlation of *CYP71A13* expression with *PAD3* led us to

Table 1. Ratios of mRNA Levels in *P. syringae*–Infected Mutant Plants Relative to Infected Wild-Type Plants Determined by qRT-PCR

		Gene		
Genotype	HAI[a]	*PAD3*	*CYP71A13*	*CYP79B2*
dde2	0	0.650	0.280	0.33
	6	1.910	1.860	0.38
	9	1.350	1.120	1.52
	24	1.520	1.150	1.32
ein2	0	0.460	0.210	0.92
	6	1.360	1.350	0.67
	9	**0.330**	**0.400**	0.96
	24	0.930	0.740	1.04
pad2	0	0.370	0.150	1.02
	6	**0.430**	**0.230**	0.87
	9	**0.360**	**0.180**	0.63
	24	1.730	0.880	1.64
pad4	0	0.190	0.170	1.02
	6	**0.190**	**0.280**	0.66
	9	**0.077**	**0.057**	**0.45**
	24	1.000	0.720	0.49
sid2	0	0.110	0.240	0.55
	6	**0.390**	**0.430**	0.73
	9	**0.110**	**0.028**	0.60
	24	**2.260**	**2.270**	1.95

Data from qRT-PCR analysis of three biologically independent experiments, each consisting of three replicate samples. Ratios <0.5 or >2 for which the difference between wild-type and mutant is statistically significant by Duncan's multiple range test ($P < 0.01$) are shown in bold.
[a] HAI, hours after infection.

investigate whether the enzyme was involved in the biosynthesis of camalexin. We hypothesized that CYP71A13 would metabolize IAOx, as it belongs to the CYP71 family, whose members include the oxime-metabolizing P450s CYP71E1, involved in dhurrin biosynthesis, as well as CYP83A1 and CYP83B1, involved in glucosinolate biosynthesis (Bak et al., 1998b, 2001; Hansen et al., 2001; Naur et al., 2003). Historically, the CYP83s were assigned to their own family based on a short EST sequence. They have since been assigned to the CYP71 family based on similarity of the full-length sequences.

CYP71A13 was heterologously expressed in *Escherichia coli* to test it for the ability to metabolize IAOx. The coding region of *CYP71A13* was PCR amplified from cDNA generated from rosette leaves and cloned into the expression vector pSP19g10L, which is optimized for expression of cytochromes P450 in *E. coli* (Barnes et al., 1991). The construct consisted of the CDS of *CYP71A13* except that the second codon, for Gly, was changed to an Ala codon, which is preferred for expression in *E. coli* (Barnes et al., 1991). CYP71A13 was functionally expressed in *E. coli* as evidenced by a carbon monoxide difference spectrum with the characteristic peak of 450 nm, as shown in Figure 6 (Omura and Sato, 1964). Based on the peak at 450 nm, the expression level of CYP71A13 was estimated to be 500 nmol cytochrome P450 (liter of culture)$^{-1}$. When spheroplasts from *E. coli* expressing CYP71A13 were reconstituted in lipid micelles with recombinant NADPH-cytochrome P450-reductase from *Arabidopsis* (ATR1) and fed with IAOx, a compound accumulated in the reaction mixture, as shown by the liquid chromatography–mass spectrometry (LC-MS) spectra in Figure 7. LC-MS analysis showed that the compound was IAN based on comparison to an authentic standard (Figure 7). This result shows that CYP71A13 catalyzes the dehydration of IAOx to IAN.

IAN did not accumulate in reaction mixtures with spheroplasts from *E. coli* carrying the empty vector (Figure 7). Although product formation was strictly dependent on CYP71A13, it was not always dependent on exogenous NADPH or reductase.

Spectral Characterization of Recombinant CYP71A13

We analyzed the binding of different compounds to the active site of CYP71A13 spectroscopically (Schenkman et al., 1967). Detection of direct binding of oximes to P450 enzymes has been reported to be difficult (Boucher et al., 1994; Kahn et al., 1999; Bak et al., 2001). As an alternative method that has been applied in similar situations, we tested if the binding of substrate could be measured as the ability to displace tryptamine from the active site (Jefcoate, 1978; Bak et al., 2001). Figure 8 shows that addition of tryptamine to recombinant CYP71A13 resulted in the formation of a typical type II spectrum, typically seen for amines. The spectrum was gradually reversed by addition of increasing concentrations of IAOx, resulting in a reverse type II spectrum (Figure 8). The minimum concentration of IAOx required to displace tryptamine was 2.5 μM, showing that low concentrations of IAOx can displace tryptamine from the active site. Displacement of tryptamine was also observed after addition of phenylacetaldoxime (Figure 8). However, under the conditions used, the amplitude of the reverse type II spectrum was not as

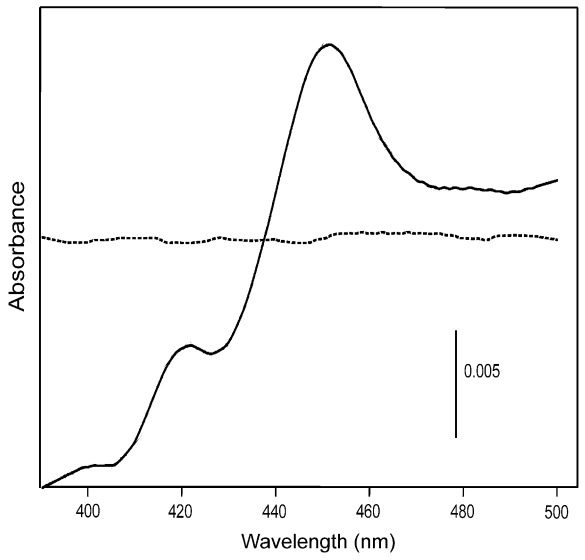

Figure 6. Carbon Monoxide Difference Spectrum of CYP71A13.

CYP71A13 was functionally expressed in *E. coli* as observed by the CO-difference spectrum of purified membranes. The dotted and solid lines represent the spectrum before and 15 min after CO exposure. The spectra were recorded at room temperature.

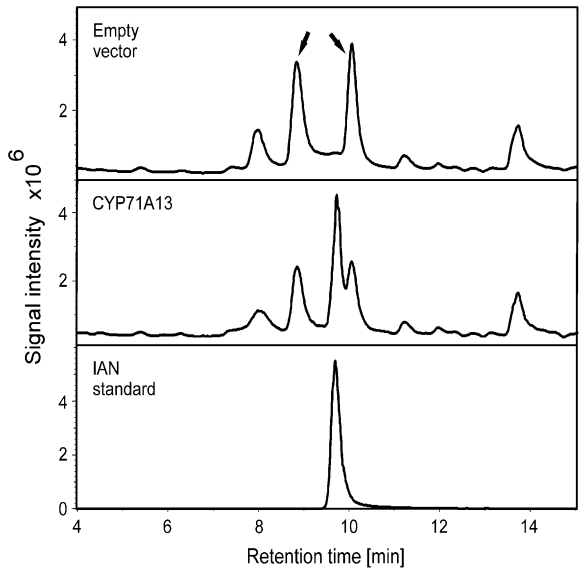

Figure 7. The Catalytic Properties of CYP71A13 toward IAOx as Analyzed by LC-MS.

LC-MS chromatograms from *E. coli* spheroplasts reconstituted with recombinant NADPH:cytochrome P450 reductase from *Arabidopsis* (ATR1) and incubated with IAOx. The reaction mixtures were extracted with ethyl acetate, and the organic phase was analyzed by LC-MS. IAOx is indicated by arrows. The two geometric isomers appear as separate peaks but with an elevated baseline in between due to partial on-column equilibration.

strong as with IAOx even at higher substrate concentrations, suggesting that phenylacetaldoxime is not as good of a substrate as IAOx since amplitude of the spectrum has been correlated with rate of turnover (Kahn et al., 1999). Neither the Tyr-derived oxime, *p*-hydroxyphenylacetaldoxime, nor IAN displaced the inhibitor (data not shown).

Transient Expression of CYP71A13 in Tobacco

To determine whether CYP71A13 converts IAOx to IAN in plants, we expressed CYP71A13 together with CYP79B2 transiently in tobacco (*Nicotiana benthamiana*) plants. We took advantage of the fact that several enzymes can be transiently coexpressed in high amounts in tobacco cells in the presence of the suppressor of silencing, p19 (Voinnet et al., 2003). Tobacco plants were infiltrated with *Agrobacterium tumefaciens* transformed with expression constructs of CYP79B2, CYP71A13, or both. In all cases, the suppressor of silencing construct, p19, was coinfiltrated. The expression of *CYP79B2* and *CYP71A13* were driven by the 35S promoter. No CYP79 homologs have been identified in tobacco (Bak et al., 1998a), and neither IAOx nor IAN has been reported. When microsomes were incubated with Trp, IAOx was detected in reaction mixtures with microsomes from plants expressing CYP79B2, whereas both IAOx and IAN were detected in reaction mixtures with microsomes from plants expressing CYP79B2 and CYP71A13, as shown in Figure 9. Neither IAOx nor IAN was detected in reaction mixtures from microsomes expressing p19. These results show that recombinant CYP71A13 expressed in *E. coli* or in plant cells can catalyze the dehydration of IAOx to IAN in vitro.

The Role of IAN in Camalexin Biosynthesis

In vivo feeding of IAN to camalexin biosynthetic mutants was performed to address the question of whether IAN is a precursor

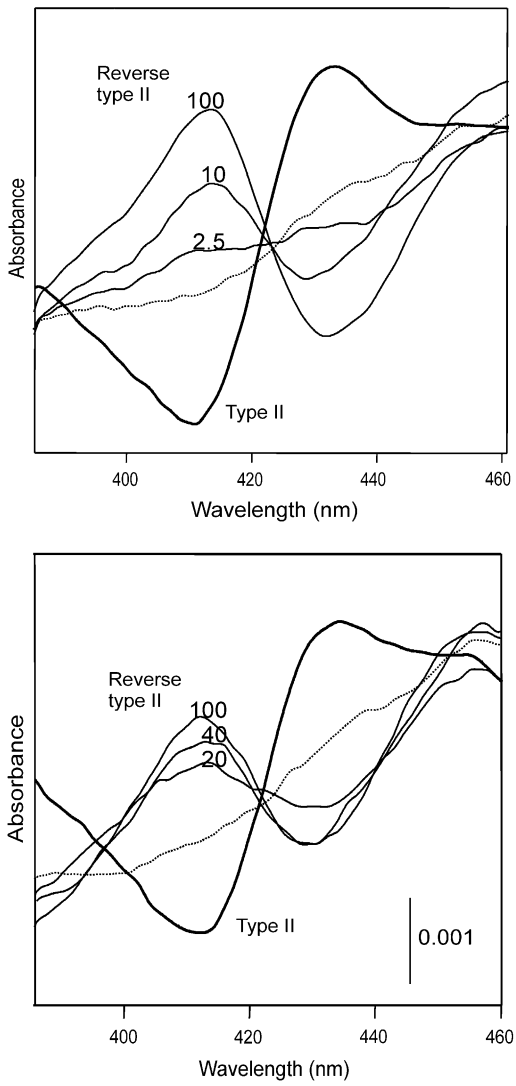

Figure 8. Analysis of CYP71A13 by Optical Difference Spectroscopy.

A saturated type II spectrum was obtained with 100 μM tryptamine in the sample cuvette (thick solid line). The addition of 100 μM tryptamine to the reference cuvette gave a baseline (dotted line). The spectra were recorded at room temperature and did not increase over time.

(A) Increasing concentrations of IAOx in the sample cuvette (2.5, 10, and 100 μM) gradually displaced tryptamine, giving the reverse type II spectrum.

(B) Increasing concentrations of phenylacetaldoxime in the sample cuvette (20, 40, and 100 μM) gradually displaced tryptamine, giving the reverse type II spectrum.

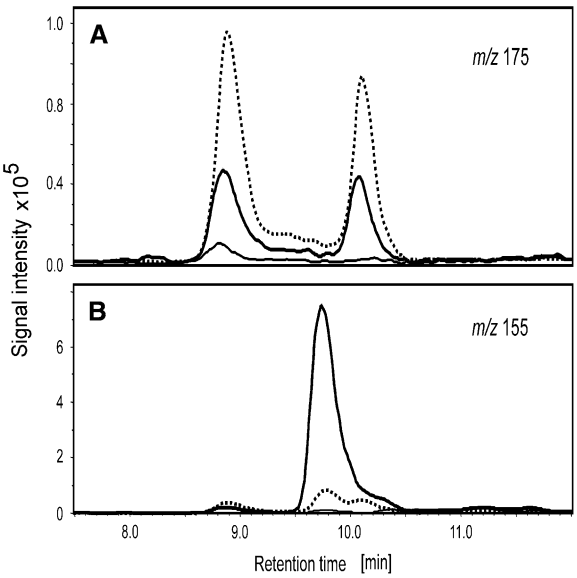

Figure 9. Transient Expression of *CYP79B2* and *CYP71A13* in *N. benthamiana* Results in Conversion of Trp to IAN via IAOx.

Microsomes from leaves infiltrated with p19 (thin solid line), *CYP79B2* (dotted line), or *CYP79B2* and *CYP71A13* (thick solid line) in combination with p19 were incubated with Trp. After incubation, the reaction mixtures were extracted with ethyl acetate, and the organic phases were analyzed by LC-MS. *m/z*, mass-to-charge ratio.

(A) Reconstructed ion chromatogram of *m/z* 175 (IAOx) from the different microsomal assays.

(B) Reconstructed ion chromatogram of *m/z* 155 (IAN) from the different microsomal assays.

in the camalexin pathway. Figure 10 shows that when IAN was applied to silver nitrate–treated *cyp71A13* leaves, camalexin levels were approximately sixfold higher than when water was applied. Similarly, IAN treatment restored camalexin synthesis in *cyp79B2 cyp79B3* plants that are unable to produce camalexin due to failure to synthesize IAOx (Glawischnig et al., 2004). By contrast, the camalexin deficiency of *pad3* was not corrected by IAN application, consistent with PAD3 (CYP71B15) catalyzing the final step in camalexin biosynthesis (Schuhegger et al., 2006). These results are in accordance with the idea that IAN is an intermediate in camalexin synthesis, and the reduced camalexin synthesis in *cyp71A13* mutants results from inadequate IAN production.

DISCUSSION

We have shown that CYP71A13 is required for pathogen-induced camalexin synthesis in *Arabidopsis* and that like camalexin-deficient *pad3* mutants, *cyp71A13* mutants are susceptible to *A. brassicicola*. We found that CYP71A13 catalyzes the first committed step in camalexin biosynthesis by dehydrating IAOx to IAN as evidenced by biochemical characterization of recombinant CYP71A13. In addition, we have shown that the *cyp71A13* knockout phenotype can be restored by in vivo feeding with IAN, strongly suggesting that IAN is an intermediate in camalexin biosynthesis.

The Role of Camalexin in Disease Resistance

After identification of *PAD3* as *CYP71B15*, the disease phenotypes of *pad3* plants were taken as an indication of whether or not camalexin is important for resistance to various pathogens. However, there remained a small possibility that these conclusions were incorrect due to other possible activities of PAD3, antimicrobial activity of the PAD3 substrate, or other unanticipated effects of the mutation. Our observation that *cyp71A13* and *pad3* mutants are unaffected in resistance to *P. syringae* and are dramatically more susceptible to *A. brassicicola* substantially strengthens the conclusion that camalexin does not play a major role in resistance to *P. syringae* but is very important for resistance to *A. brassicicola* (Glazebrook and Ausubel, 1994; Thomma et al., 1999).

Regulation of Camalexin Synthesis

We found that mRNA levels of both *PAD3* and *CYP71A13* are greatly increased in response to *P. syringae* infection. Expression of these two genes is tightly correlated over a large number of microarray experiments and similarly affected by mutations in canonical defense regulatory genes. This suggests that it might be possible to identify the missing enzymes in camalexin

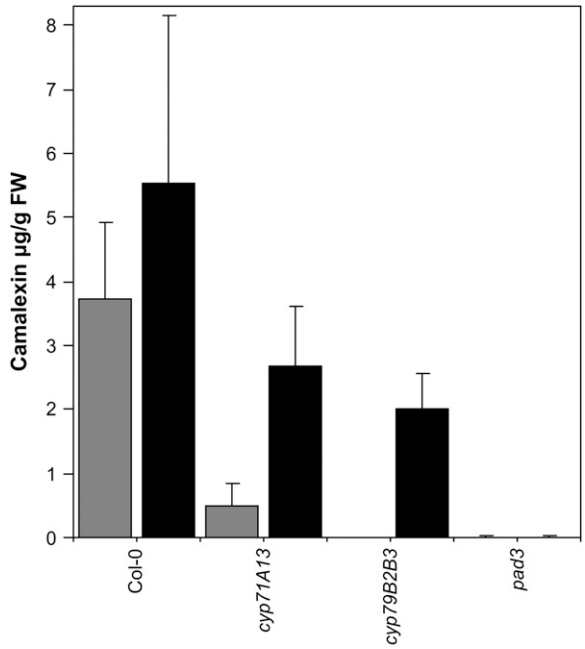

Figure 10. In Vivo Feeding of IAN to $AgNO_3$-Treated *Arabidopsis* Mutants.

After spraying with silver nitrate, rosette leaves of Col-0, *cyp71A13-1*, *cyp79B2 cyp79B3*, and *pad3* plants were incubated with 250 μM IAN (black bars) or water (gray bars). Bars represent means and SD of six replicates. Significance of differences between water- and IAN-treated plants was tested using an unpaired, two-tailed *t* test. The difference for Col-0 was not significant ($P = 0.16$), while the differences for *cyp71A13-1* and *cyp79B2 cyp79B3* were highly significant ($P = 0.00028$ and 0.0000049, respectively).

synthesis by searching for genes coregulated with *PAD3* and *CYP71A13*. However, we have not found other genes as tightly coregulated with *PAD3* and *CYP71A13* as they are with each other, and some testing of candidate genes has not yet yielded additional camalexin-deficient mutants. Perhaps the missing enzymes participate in biosynthetic processes in addition to camalexin synthesis and so do not show tight coregulation, as is the case with *CYP79B2*. Alternatively, they may be absent from the ATH1 array, which does not include probes for every presently annotated *Arabidopsis* gene.

We observed coregulated expression of *PAD3* and *CYP71A13* in a set of defense signaling mutants. Expression of *PAD3* and *CYP71A13* was transiently reduced in *ein2*, *pad2*, *pad4*, and *sid2* mutants. Among these, *ein2*, *pad2*, and *pad4* display reduced camalexin levels. *PAD2* encodes γ-glutamyl cysteine synthase, which is required for synthesis of glutathione (Parisy et al., 2007). Glutathione levels in *pad2* plants are reduced, while cysteine levels are fivefold higher than in the wild type. Based on in vivo feeding studies, Zook and Hammerschmidt (1997) proposed that cysteine is the sulfur donor for camalexin, but perhaps the sulfur donor is actually glutathione. Glutathione is also involved in regulation of NPR1 activity through redox changes (Mou et al., 2003). Thus, the camalexin deficiency of *pad2* plants may result from causes other than or in addition to the reduced expression of *PAD3* and *CYP71A13. PAD4* encodes a regulator that affects expression of many defense-related genes (Jirage et al., 1999; Glazebrook et al., 2003). The phenotypes of *sid2* plants are difficult to explain. While the impact of *sid2* on expression of *PAD3* and *CYP71A13* at 9 h after infection is comparable to that of *pad4*, there is no reduction of camalexin in *sid2* plants (Nawrath and Metraux, 1999). Perhaps a more detailed time course would show that the depression of *PAD3* and *CYP71A13* is more transient in *sid2* than in *pad4* plants. None of the mutations studied compromised expression of *PAD3* or *CYP71A13* at 24 h after infection, so even though there is a requirement for SA signaling at early times, some other signaling process must be sufficient for wild-type expression levels at later time points. It seems likely that regulation of camalexin synthesis involves the action of multiple regulatory factors and that a complete understanding will require considerably more work.

CYP71A13 Converts IAOx to IAN

CYP71A13 expressed in *E. coli* and in leaves of *N. benthamiana* metabolized IAOx to IAN. In *E. coli* spheroplasts, the dehydration of IAOx was not dependent on exogenous P450 reductase, which suggests that the reaction could be supported by the endogenous *E. coli* flavodoxin/NADPH-flavodoxin reductase system, which can support other heterologously expressed P450 enzymes (Jenkins and Waterman, 1994; Halkier et al., 1995). Furthermore, the IAN formation was not always dependent on exogenous NADPH, suggesting that residual amounts of NADPH may occasionally be present in the spheroplast preparation. For P450-catalyzed dehydration of oximes, it has been suggested that once NADPH reduces cytochrome P450 to the ferrous state, the reaction proceeds without further action by NADPH (DeMaster et al., 1992). Similar conditions might apply to CYP71A13. Dehydration of oxime to nitrile is not a redox reaction and therefore not a typical P450-catalyzed reaction. However, other P450s have been shown to catalyze dehydration reactions, including members of the CYP3A family (Boucher et al., 1994; Mathews et al., 1998) and the multifunctional CYP71E1 (Bak et al., 1998b).

The substrate binding spectra showed that oximes derived from Trp and Phe, but not Tyr, could displace tryptamine from the active site of CYP71A13. This indicates that the range of compounds that fit into the substrate binding pocket is limited. The spectral data are in accordance with reconstitution experiments with labeled oximes, in which IAOx, but not the Tyr-derived *p*-hydroxyphenylacetaldoxime, was metabolized by CYP71A13. The binding of phenylacetaldoxime to the active site of CYP71A13 indicates that this compound is a substrate for the enzyme, although it remains to be determined whether it can be metabolized.

In the biosynthesis of the Tyr-derived cyanogenic glucoside dhurrrin in *Sorghum bicolor*, CYP71E1 catalyzes the metabolism of *p*-hydroxyphenylacetaldoxime to the corresponding hydroxynitrile, *p*-hydroxyphenylmandelonitrile, via a nitrile intermediate (Bak et al., 1998b; Kahn et al., 1999). Both oxime and nitrile fed to sorghum microsomes or to micelles with recombinant CYP71E1 reconstituted with sorghum reductase were converted to the hydroxynitrile. Reconstitution of recombinant CYP71E1 with *E. coli* flavodoxin/NADPH-flavodoxin reductase drove the reaction only to the corresponding nitrile, *p*-hydroxyphenylacetonitrile, suggesting a specific redox requirement (Bak et al., 1998b). In our study, IAN was the only product formed when IAOx was incubated with recombinant CYP71A13 from either *E. coli* or tobacco. In contrast with CYP71E1 in the cyanogenic pathway, CYP71A13 was not able to metabolize IAN further. The role of IAN as a product of CYP71A13 in plants was supported by the ability of exogenous IAN to rescue the camalexin-deficient phenotype of *cyp71A13* knockout mutants.

When tobacco microsomes were incubated with Trp, IAN accumulated in reaction mixtures from plants expressing CYP79B2 and CYP71A13. In addition, trace amounts of IAN were observed in reaction mixtures from plants that expressed CYP79B2, whereas no IAN was observed in the reaction mixture from plants expressing the control, p19. This suggests that tobacco can convert some of the accumulated IAOx to IAN. We do not know whether this occurs enzymatically or nonenzymatically.

IAOx constitutes a metabolic branch point among indole glucosinolates, camalexin, and IAA biosynthesis. How these pathways are organized and regulated around IAOx is currently unclear (Hansen and Halkier, 2005). However, as camalexin is produced only under inducing conditions, IAOx is presumed to be funneled into indole glucosinolates under normal conditions (Bak et al., 2001).

IAN in Camalexin Biosynthesis

The role of IAN as an intermediate in camalexin biosynthesis was supported by the ability of exogenous IAN to rescue the camalexin-deficient phenotype of *cyp71A13* knockout mutants. Plants overexpressing *CYP79B2* or *PAD3* did not have increased accumulation of camalexin (Glawischnig et al., 2004; Schuhegger et al., 2006). The photosynthetic mutant *dgd1* (Dörmann et al.,

1995), which contains 45-fold elevated levels of IAN (Fiehn et al., 2000), does not accumulate more camalexin than the wild type in response to silver nitrate (R. Schuhegger and E. Glawischnig, unpublished data). Thus, the rate-limiting step in camalexin synthesis is unclear. Whether IAN functions as an intermediate in the biosynthesis of other IAOx-derived phytoalexins from *Brassica* remains to be investigated. IAN has been recognized as a phytoalexin that is induced upon fungus attack in *Brassica juncea* (Pedras et al., 2002).

IAN and Auxin

Our data show that IAN produced by CYP71A13 is an intermediate in the biosynthesis of camalexin. In addition, IAN has often been suggested as an intermediate in IAA biosynthesis in crucifers (reviewed in Pollmann et al., 2006) and also in maize (*Zea mays*), a plant that does not produce camalexin or indole glucosinolates (Park et al., 2003). Auxin biosynthesis via IAN requires the action of nitrilases (NIT1-3) that hydrolyze IAN to IAA (Bartling et al., 1992). Generally, nitrilases have K_m values for IAN in the millimolar range (Vorwerk et al., 2001), indicating that IAN is not a very good substrate. Nevertheless, *nit1* plants did not show the auxin effect seen in wild-type plants upon treatment with exogenous IAN (Normanly et al., 1997), and NIT2-overexpressing lines from *Arabidopsis* and tobacco show increased sensitivity to exogenous IAN (Schmidt et al., 1996; Normanly et al., 1997). However, attempts to rescue the high-auxin phenotype of *sur2* by crossing *sur2* to *nit1-1* were unsuccessful (Bak et al., 2001), raising further questions about the role of IAN in auxin biosynthesis.

IAN might be an intermediate in both camalexin and auxin biosynthesis, suggesting that either the IAN-metabolizing enzymes are competing for substrate or IAN is highly channeled within each pathway (i.e., IAN is produced and metabolized in situ). Alternatively, IAN is primarily involved in camalexin biosynthesis and only converted to IAA when excess IAN accumulates. The latter idea may explain why the expression of *NIT1* and *NIT2* is induced by exogenous IAN (Grsic et al., 1998). Another source of IAN is the turnover of indole glucosinolates (Bones and Rossiter, 2006). A basal level of IAN is present in healthy plants (Ilic et al., 1996).

Camalexin Biosynthesis Downstream of IAN

So far, the metabolic route from IAN to dihydrocamalexic acid in camalexin biosynthesis is unknown. A proposed candidate intermediate is indole-3-carboxaldehyde (Browne et al., 1991), although this compound does not appear to be a precursor of camalexin based on in vivo feeding studies (Schuhegger et al., 2006). Further studies are needed to identify the enzymes catalyzing the conversion of IAN to dihydrocamalexic acid in the biosynthetic pathway of camalexin, the model compound for studying the bioactive cruciferous indole alkaloids.

METHODS

Plant Growth

Nicotiana benthamiana plants used for transient expression were grown at 24°C (day) and 17°C (night) in a greenhouse. For pathogen experiments, *Arabidopsis thaliana* was grown in a controlled-environment chamber at 22°C, 70% relative humidity, 12 h light (100 μM m^{-2} s^{-1} fluorescent illumination), and 12 h dark. All genotypes were in the Col-0 background. *pad3* was *pad3-1* (Glazebrook and Ausubel, 1994), *cyp79B2*, *cyp79B3*, and the double mutant were from Zhao et al. (2002), *dde2* was *dde2-2* (von Malek et al., 2002), *ein2* was *ein2-1* (Alonso et al., 1999), *pad2* was *pad2-1* (Parisy et al., 2007), *pad4* was *pad4-1* (Jirage et al., 1999), and *sid2* was *sid2-2* (Wildermuth et al., 2001).

Characterization of *cyp71A13* Mutant Alleles

Plants homozygous for *cyp71A13-1* and *cyp71A13-2* were identified by PCR as described (Sessions et al., 2002). For *cyp71A13-1*, gene-specific primers were 5′-CGAGTAGAGTTGCGTTGGGAAGA-3′ (105136LP) and 5′-CCATGTGGCCTAATAGTTGACCG-3′ (105136RP), while the T-DNA left border primer was 5′-GGAACAACACTCAACCCTATCTCG-3′ (LBe). For *cyp71A13-2*, gene-specific primers were 5′-TTCTCCATAGGGAGCAAACAC-3′ (505E09LP) and 5′-TGACGTCCTGCACTATTGACA-3′ (505E09RP), while the T-DNA left border primer was 5′-TTCATAACCAATCTCGATACAC-3′ (LB3). The positions of the T-DNA insertions were determined by DNA sequencing of the PCR products obtained with primers LBe and 105136RP (for *cyp71A13-1*), and LB3 and 505E09 (for *cyp71A13-2*).

Infection with Pathogens

Infection with *Pseudomonas syringae* strain *Psm* ES4326 and determination of bacterial growth was as described (Parisy et al., 2007). Infection with *Alternaria brassicicola* strain ATCC 96866 was achieved by placing 10-μL droplets of water containing 10^5 spores/mL of water onto the abaxial surface of the third, fourth, and fifth true leaves of 3-week-old plants. Plants were kept tightly covered for the first day, and symptoms were assessed after 3 d. Camalexin in pathogen-infected plants was determined as described (Glazebrook and Ausubel, 1994).

Determination of Expression Levels

For ATH1 microarray analysis, wild-type Col-0 plants were infected with *Psm* ES4326 by syringe infiltration to a starting bacterial titer of 10^4 colony-forming units/cm^2 of leaves ($OD_{600} = 0.002$) or mock-infected and sampled after 9, 24, or 32 h. Three independent experiments were performed. RNA was purified using Trizol reagent (Invitrogen) according to the manufacturer's instructions with modifications for tissues with high starch content. Labeled cRNA was produced using the Affymetrix one-cycle target labeling kit (Affymetrix). Raw data were converted to expression values for each gene using robust multichip average (Irizarry et al., 2003). Complete data sets are available from the Nottingham Arabidopsis Stock Centre (accession number NASCARRAYS-414; http://affymetrix.arabidopsis.info/). The values shown in Figure 5 were obtained by combining the expression values from the three replicate data sets to obtain the means and the standard deviations.

For qRT-PCR analysis, plants were infected as above and sampled immediately or 6, 9, or 24 h later. Total RNA was isolated using TRIzol (Invitrogen) following the manufacturer's protocol. qRT-PCR was performed using the Superscript III Platinum SYBR Green One-Step qRT-PCR kit (Invitrogen) and the Applied Biosystems 7500 Real Time PCR machine. The thermal cycling program was as follows: 50°C for 10 min and 95°C for 10 min, followed by 40 cycles of 95°C for 15 s, 60°C for 1 min, and a one-cycle dissociation stage at 95°C for 15 s, 60°C for 1 min, and 95°C for 15 s. The primers were as follows: *Actin2* (At3g18780), 5′-AGTGTCTGGATCGGTGGTTC-3′ and 5′-CCCCAGCTTTTTAAGCCTTT-3′; *PAD3* (At3g26830), 5′-TGCTCCCAAGACAGACAATG-3′ and 5′-GTTTTGGATCACGACCCATC-3′; CYP71A13 (At2g30770), 5′-TAAAGAGGTGCTTCGGTTGC-3′ and 5′-TATCGCAGTGTCTCGTTGGA-3′;

and CYP79B2 (At4g39950), 5′-GTTTCTGGCTAAACCGTTGG-3′ and 5′-TCTGGTAACCGGAATTGACC-3′. Actin2 was used as the internal reference gene. Samples from each of three biological replicates were assayed in triplicate, for a total of nine measurements per data point. Expression values were normalized to those of *actin2*. Data were then subjected to analysis of variance in a completely randomized design, and the treatment means separated by Duncan's multiple range test. The values in Supplemental Table 2 online are the means and standard deviations from all nine measurements per data point.

Synthesis of IAOx

IAOx was synthesized from indole-3-acetaldehyde as described (Rausch et al., 1985). The structure was verified by nuclear magnetic resonance.

Heterologous Expression of CYP71A13 in *Escherichia coli*

The coding sequence of CYP71A13 (NM 128630.2; www.ncbi.nlm.nih.gov) was amplified from cDNA with the following primers: forward, 5′-TACGCCATATGGCAAATATTCAAGAAATGGAAATGATATTGAGTA-3′; reverse, 5′-AATAACAAAGCTTACACAACCGAAGATGGAAA-3′. The primers introduce 5′ *Nde*I and 3′ *Hin*dIII sites (underlined), which were used to clone the fragment into *Nde*I/*Hin*dIII-digested pSP19g10L (Barnes et al., 1991). The forward primer changes the second codon from Gly to Ala (in italics). The expression construct was transformed into *E. coli* strain C43 (DE3). For expression of CYP71A13, one colony was grown overnight in Luria-Bertani medium + ampicillin (100 μg/mL), and 1 mL of the culture was used to inoculate 100 mL of modified terrific broth medium, pH 7.5, with 100 μg/mL of ampicillin, 1 mM isopropylthio-β-galactoside, 1 mM δ-aminolevulinic acid, and 1 mM thiamine. The culture was grown at 28°C at 110 rpm for 40 h. Spheroplasts were made in accordance with Halkier et al. (1995), except that glycerol was omitted from the final buffer. A Triton X-114–induced phase partitioning was done as described previously (Halkier et al., 1995).

Measurement of Carbon Monoxide Difference Spectrum

CYP71A13 (0.24 μM) dissolved in 50 mM KPi, pH 7.9, with a few grains of solid sodium dithionite was distributed in two cuvettes. When a stable baseline was obtained, the sample cuvette was bubbled with CO (30 s), and spectral changes were recorded for 15 min on a Lambda 800 UV-Vis spectrophotometer (Perkin-Elmer) at room temperature. The amount of expressed functional cytochrome P450 was monitored by Fe^{2+}·CO versus Fe^{2+} difference spectroscopy and quantified using an extinction coefficient of 91 mM^{-1} cm^{-1}.

Reconstitution of Functional CYP71A13

The activity of CYP71A13 was measured by reconstituting spheroplasts from *E. coli* expressing CYP71A13 with recombinant NADPH:cytochrome P450 reductase from *Arabidopsis* (ATR1). The *Arabidopsis* NADPH:cytochrome P450 reductase was expressed and purified as described previously (Naur et al., 2003). For a typical reconstitution experiment, 5 μL of CYP71A13 was incubated with 5 μL (10 to 20 units) NADPH-cytochrome P450 reductase from *Arabidopsis*, ATR1, 5 μL ^{14}C-substrate, 25 μg dilauroyl phosphatidyl choline, and 3 mM NADPH in 50 mM KPi, pH 7.9, in a total volume of 50 μL. The reactions were incubated at 30°C for 1 h. For LC-MS analysis, 5× 50-μL reaction mixtures were made as above, except 200 μM cold IAOx was used in place of ^{14}C-labeled IAOx. The reactions were extracted with 200 μM ethyl acetate; the ethyl acetate phases were combined, dried in vacuo, and resuspended in 50 μL 50% ethanol.

Substrate Binding Spectra

CYP71A13 (0.1 μM) dissolved in 50 mM KPi, pH 7.9, was distributed in two cuvettes. The reverse type II spectrum was obtained by adding 100 μM tryptamine to the sample cuvette. The spectral change was recorded, and 100 μM tryptamine was added to a reference cuvette, giving a baseline. IAOx was titrated (2.5 to 100 μM) to the sample cuvette. An equal amount of solvent (50% ethanol) was added to the reference cuvette. Curves for CO spectrum and binding spectra were plotted and smoothed using SigmaPlot 2001 software (Systat Software).

LC-MS Analysis

LC-MS was performed using a HP1100 liquid chromatograph (Agilent Technologies) coupled to a Bruker Esquire 3000+ ion trap mass spectrometer (Bruker Daltonics). An XTerra MS C18 column (Waters; 3.5 μM, 2.1 × 100 mm) was used at a flow rate of 0.2 mL min^{-1}. The mobile phases were as follows: A, 0.1% (v/v) HCOOH; B, methanol. The gradient program was as follows: 0 to 2 min, isocratic 35% B; 2 to 20 min, linear gradient 35 to 100% B; 20 to 25 min, isocratic 100% B. The column temperature was kept at 20°C. The spectrometer was run in atmospheric pressure chemical ionization mode, and positive ions were observed.

Transient Expression of CYP71A13 in *N. benthamiana*

The coding sequence of CYP71A13 was amplified from cDNA (Mikkelsen et al., 2003) with the following primers: forward, 5′-GGCTTAAUATGAGCAATATTCAAGAAAATGGA-3′; reverse, 5′-CCTTTAAUTTACACAACCGAAGATGGAAA-3′. The coding sequence of CYP79B2 was amplified with the following primers: forward, 5′-GGCTTAAUATGAACACTTTTACCTCAAACTCT-3′; reverse, 5′-GGTTTAAUTCACTTCACCGTCGGGTAGAGAT-3′. The sequences were cloned with the USER technology (Nour-Eldin et al., 2006) into USER-compatible pCAMBIA1300 (CYP71A13) or pCAMBIA2300 (CYP79B2) vectors, where expression was driven by the 35S promoter. The constructs were transformed into *Agrobacterium* strain C58 and grown overnight in YEP with the appropriate antibiotics (p19, kanamycin + tetracycline; CYP71A13 and CYP79B2, kanamycin + rifampicin), pelleted by centrifugation, and resuspended in 10 mM MES, 10 mM $MgCl_2$, and 100 μM acetosyringone to OD 0.5 to 0.8 and left shaking at room temperature for 3 h. Three-week-old tobacco leaves were infiltrated with a given expression construct in combination with the suppressor of silencing, p19 (Voinnet et al., 2003) in a ratio of 3:1. When several expression constructs were used in combination with p19, the ratio was equal among all constructs used.

Microsomal Preparation from Tobacco Leaves

Microsomes were made 4 d after infiltration according to Porchia et al. (2002). Briefly, tobacco leaves were homogenized with a polytron in homogenization buffer (50 mM KPi, pH 7.2, 400 mM sucrose, 4 mM DTT, and Complete proteinase inhibitor cocktail [Roche]) and filtered through muslin. Tissue was pelleted by centrifugation at 5000*g* for 15 min, and the supernatant was centrifuged at 50,000*g* for 45 min. The microsomes were resuspended in homogenization buffer and homogenized, and glycerol was added to a final concentration of 15%. To measure CYP71A13 activity, ~35-μL microsomes (equal amount of protein) were incubated in a total volume of 50 μL with 200 μM substrate and 3 mM NADPH at 30 C for 1 h. The reaction mixture was extracted with 200 μL ethyl acetate. The organic phases were dried under vacuum and resuspended in 50% ethanol. For structural analysis, five reaction mixtures were combined and resuspended in 50 μL 50% ethanol.

In Vivo Feeding of IAN to *Arabidopsis* Mutants

The Col-0 wild type, *cyp71A13*, and *cyp79B2 cyp79B3* knockout, as well as *pad3* mutants, were sprayed with 5 mM silver nitrate to test

complementation of the pathway with IAN. After 8 h, rosette leaves were excised at the petiole and incubated in 200 μL 250 μM IAN or water for an additional 16 h. Camalexin was extracted and quantified as described (Schuhegger et al., 2006).

Accession Numbers

Sequence data for genes from this article can be found in the GenBank/EMBL data libraries under the following Arabidopsis Genome Initiative identifiers: CYP71A13 (At2g30770), CYP71A12 (At2g30750), CYP79B2 (At4g39950), CYP79B3 (At2g22330), and PAD3 (At3g26830).

Supplemental Data

The following materials are available in the online version of this article.

Supplemental Figure 1. A Mutation in CYP71A12 (At2g30750) Does Not Cause Camalexin Deficiency.

Supplemental Figure 2. Mutations in Camalexin Biosynthetic Genes Do Not Cause Enhanced Susceptibility to *P. syringae*.

Supplemental Figure 3. Camalexin Biosynthetic Pathway.

Supplemental Table 1. Genevestigator Data for Expression Levels of *PAD3* (At3g26830), *CYP71A13* (At2g30770), *CYP79B2* (At4g39950), *CYP79B3* (At2g22330), and *CYP71A12* (At2g30750).

Supplemental Table 2. Quantitative RT-PCR Mean Expression Values for *PAD3*, *CYP71A13*, and *CYP79B2* after Infection with *P. syringae*.

ACKNOWLEDGMENTS

We thank Joanne Chory for *cyp79B2*, *cyp79B3*, and *cyp79B2 cyp79B3* seed, Fred Ausubel for *sid2-2*, Beat Keller for *dde2-2*, and the ABRC for SALK T-DNA lines. ATH1 microarray data were provided by Raka Mitra. This project was initiated by J.G. and S.G. at the Torrey Mesa Research Institute with funding from Syngenta. Support to J.G. and E.G. was from Grant DE-FG02-05ER15670 from the Department of Energy Biosciences and from Grant GL346/1 from the Deutsche Forschungsgemeinschaft, respectively. M.N. thanks the Royal Veterinary and Agricultural University for a PhD stipend.

Received February 26, 2007; revised May 9, 2007; accepted May 29, 2007; published June 15, 2007.

REFERENCES

Alonso, J.M., Hirayama, T., Roman, G., Nourizadeh, S., and Ecker, J.R. (1999). *EIN2*, a bifunctional transducer of ethylene and stress responses in Arabidopsis. Science **284:** 2148–2152.

Alonso, J.M., et al. (2003). Genome-wide insertional mutagenesis of *Arabidopsis thaliana*. Science **301:** 653–657.

Bak, S., Kahn, R., Nielsen, H., Møller, B., and Halkier, B. (1998b). Cloning of three A-type cytochromes P450, CYP71E1, CYP98, and CYP99 from *Sorghum bicolor* (L.) Moench by a PCR approach and identification by expression in *Escherichia coli* of CYP71E1 as a multifunctional cytochrome P450 in the biosynthesis of the cyanogenic glucoside dhurrin. Plant Mol. Biol. **36:** 393–405.

Bak, S., Nielsen, H., and Halkier, B. (1998a). The presence of CYP79 homologues in glucosinolate-producing plants shows evolutionary conservation of the enzymes in the conversion of amino acid to aldoxime in the biosynthesis of cyanogenic glucosides and glucosinolates. Plant Mol. Biol. **38:** 725–734.

Bak, S., Tax, F.E., Feldmann, K.A., Galbraith, D.W., and Feyereisen, R. (2001). CYP83B1, a cytochrome P450 at the metabolic branch point in auxin and indole glucosinolate biosynthesis in Arabidopsis. Plant Cell **13:** 101–111.

Barlier, I., Kowalczyk, M., Marchant, A., Ljung, K., Bhalerao, R., Bennett, M., Sandberg, G., and Bellini, C. (2000). The SUR2 gene of *Arabidopsis thaliana* encodes the cytochrome P450 CYP83B1, a modulator of auxin homeostasis. Proc. Natl. Acad. Sci. USA **97:** 14819–14824.

Barnes, H.J., Arlotto, M.P., and Waterman, M.R. (1991). Expression and enzymatic activity of recombinant cytochrome P450 17 alpha-hydroxylase in *Escherichia coli*. Proc. Natl. Acad. Sci. USA **88:** 5597–5601.

Bartling, D., Seedorf, M., Mithofer, A., and Weiler, E.W. (1992). Cloning and expression of an Arabidopsis nitrilase which can convert indole-3-acetonitrile to the plant hormone, indole-3-acetic acid. Eur. J. Biochem. **205:** 417–424.

Bohman, S., Staal, J., Thomma, B.P., Wang, M., and Dixelius, C. (2004). Characterisation of an Arabidopsis-*Leptosphaeria maculans* pathosystem: Resistance partially requires camalexin biosynthesis and is independent of salicylic acid, ethylene and jasmonic acid signalling. Plant J. **37:** 9–20.

Bones, A.M., and Rossiter, J.T. (2006). The enzymic and chemically induced decomposition of glucosinolates. Phytochemistry **67:** 1053–1067.

Boucher, J.L., Delaforge, M., and Mansuy, D. (1994). Dehydration of alkyl- and arylaldoximes as a new cytochrome P450-catalyzed reaction: Mechanism and stereochemical characteristics. Biochemistry **33:** 7811–7818.

Browne, L.M., Conn, K.L., Ayer, W.A., and Tewari, J.P. (1991). The camalexins: New phytoalexins produced in the leaves of *Camelina sativa* (cruciferae). Tetrahedron **47:** 3909–3914.

Delarue, M., Prinsen, E., Onckelen, H.V., Caboche, M., and Bellini, C. (1998). Sur2 mutations of *Arabidopsis thaliana* define a new locus involved in the control of auxin homeostasis. Plant J. **14:** 603–611.

DeMaster, E.G., Shirota, F.N., and Nagasawa, H.T. (1992). A Beckmann-type dehydration of n-butyraldoxime catalyzed by cytochrome P-450. J. Org. Chem. **57:** 5074–5075.

Dörmann, P., Hoffmann-Benning, S., Balbo, I., and Benning, C. (1995). Isolation and characterization of an Arabidopsis mutant deficient in the thylakoid lipid digalactosyl diacylglycerol. Plant Cell **7:** 1801–1810.

Ferrari, S., Plotnikova, J.M., De Lorenzo, G., and Ausubel, F.M. (2003). Arabidopsis local resistance to *Botrytis cinerea* involves salicylic acid and camalexin and requires *EDS4* and *PAD2*, but not *SID2*, *EDS5* or *PAD4*. Plant J. **35:** 193–205.

Fiehn, O., Kopka, J., Dormann, P., Altmann, T., Trethewey, R.N., and Willmitzer, L. (2000). Metabolite profiling for plant functional genomics. Nat. Biotechnol. **18:** 1157–1161.

Glawischnig, E., Hansen, B.G., Olsen, C.E., and Halkier, B.A. (2004). Camalexin is synthesized from indole-3-acetaldoxime, a key branching point between primary and secondary metabolism in Arabidopsis. Proc. Natl. Acad. Sci. USA **101:** 8245–8250.

Glazebrook, J., and Ausubel, F.M. (1994). Isolation of phytoalexin-deficient mutants of *Arabidopsis thaliana* and characterization of their interactions with bacterial pathogens. Proc. Natl. Acad. Sci. USA **91:** 8955–8959.

Glazebrook, J., Chen, W., Estes, B., Chang, H.S., Nawrath, C., Metraux, J.P., Zhu, T., and Katagiri, F. (2003). Topology of the network integrating salicylate and jasmonate signal transduction derived from global expression phenotyping. Plant J. **34:** 217–228.

Glazebrook, J., Rogers, E.E., and Ausubel, F.M. (1996). Isolation of Arabidopsis mutants with enhanced disease susceptibility by direct screening. Genetics **143:** 973–982.

Glazebrook, J., Zook, M., Mert, F., Kagan, I., Rogers, E.E., Crute, I.R., Holub, E.B., Hammerschmidt, R., and Ausubel, F.M. (1997). Phytoalexin-deficient mutants of Arabidopsis reveal that *PAD4* encodes a regulatory factor and that four *PAD* genes contribute to downy mildew resistance. Genetics **146:** 381–392.

Grsic, S., Sauerteig, S., Neuhaus, K., Albrecht, M., Rossiter, J.T., and Ludwig-Müller, J. (1998). Physiological analysis of transgenic *Arabidopsis thaliana* plants expressing one nitrilase isoform in the sense or antisense direction. J. Plant Physiol. **153:** 446–456.

Halkier, B.A., Nielsen, H.L., Koch, B., and Møller, B.L. (1995). Purification and characterization of recombinant cytochrome P450TYR expressed at high levels in *Escherichia coli*. Arch. Biochem. Biophys. **322:** 369–377.

Hansen, B., and Halkier, B. (2005). New insight into the biosynthesis and regulation of indole compounds in *Arabidopsis thaliana*. Planta **221:** 603–606.

Hansen, C.H., Du, L., Naur, P., Olsen, C.E., Axelsen, K.B., Hick, A.J., Pickett, J.A., and Halkier, B.A. (2001). CYP83B1 Is the oxime-metabolizing enzyme in the glucosinolate pathway in Arabidopsis. J. Biol. Chem. **276:** 24790–24796.

Heck, S., Grau, T., Buchala, A., Metraux, J.P., and Nawrath, C. (2003). Genetic evidence that expression of *NahG* modifies defence pathways independent of salicylic acid biosynthesis in the Arabidopsis-*Pseudomonas syringae* pv. *tomato* interaction. Plant J. **36:** 342–352.

Hull, A.K., Vij, R., and Celenza, J.L. (2000). Arabidopsis cytochrome P450s that catalyze the first step of tryptophan-dependent indole-3-acetic acid biosynthesis. Proc. Natl. Acad. Sci. USA **97:** 2379–2384.

Ilic, N., Normanly, J., and Cohen, J.D. (1996). Quantification of free plus conjugated indoleacetic acid in Arabidopsis requires correction for the nonenzymatic conversion of indolic nitriles. Plant Physiol. **111:** 781–788.

Irizarry, R.A., Hobbs, B., Collin, F., Beazer-Barclay, Y.D., Antonellis, K.J., Scherf, U., and Speed, T.P. (2003). Exploration, normalization, and summaries of high density oligonucleotide array probe level data. Biostatistics **4:** 249–264.

Jefcoate, C.R. (1978). Measurement of substrate and inhibitor binding to microsomal cytochrome P-450 by optical-difference spectroscopy. Methods Enzymol. **52:** 258–279.

Jenkins, C.M., and Waterman, M.R. (1994). Flavodoxin and NADPH-flavodoxin reductase from *Escherichia coli* support bovine cytochrome P450c17 hydroxylase activities. J. Biol. Chem. **269:** 27401–27408.

Jirage, D., Tootle, T.L., Reuber, T.L., Frost, L.N., Feys, B.J., Parker, J.E., Ausubel, F.M., and Glazebrook, J. (1999). *Arabidopsis thaliana PAD4* encodes a lipase-like gene that is important for salicylic acid signaling. Proc. Natl. Acad. Sci. USA **96:** 13583–13588.

Kahn, R.A., Fahrendorf, T., Halkier, B.A., and Møller, B.L. (1999). Substrate specificity of the cytochrome P450 enzymes CYP79A1 and CYP71E1 involved in the biosynthesis of the cyanogenic glucoside dhurrin in *Sorghum bicolor* (L.) Moench. Arch. Biochem. Biophys. **363:** 9–18.

Kliebenstein, D.J., Rowe, H.C., and Denby, K.J. (2005). Secondary metabolites influence Arabidopsis/Botrytis interactions: Variation in host production and pathogen sensitivity. Plant J. **44:** 25–36.

Mathews, J., Black, S., and Burka, L. (1998). Disposition of butanal oxime in rat following oral, intravenous and dermal administration. Xenobiotica **28:** 767–777.

Mikkelsen, M.D., Hansen, C.H., Wittstock, U., and Halkier, B.A. (2000). Cytochrome P450 CYP79B2 from Arabidopsis catalyzes the conversion of tryptophan to indole-3-acetaldoxime, a precursor of indole glucosinolates and indole-3-acetic acid. J. Biol. Chem. **275:** 33712–33717.

Mikkelsen, M.D., Petersen, B.L., Glawischnig, E., Jensen, A.B., Andreasson, E., and Halkier, B.A. (2003). Modulation of CYP79 genes and glucosinolate profiles in Arabidopsis by defense signaling pathways. Plant Physiol. **131:** 298–308.

Mou, Z., Fan, W., and Dong, X. (2003). Inducers of plant systemic acquired resistance regulate NPR1 function through redox changes. Cell **113:** 935–944.

Naur, P., Petersen, B.L., Mikkelsen, M.D., Bak, S., Rasmussen, H., Olsen, C.E., and Halkier, B.A. (2003). CYP83A1 and CYP83B1, two nonredundant cytochrome P450 enzymes metabolizing oximes in the biosynthesis of glucosinolates in Arabidopsis. Plant Physiol. **133:** 63–72.

Nawrath, C., and Metraux, J.P. (1999). Salicylic acid induction-deficient mutants of Arabidopsis express PR-2 and PR-5 and accumulate high levels of camalexin after pathogen inoculation. Plant Cell **11:** 1393–1404.

Normanly, J., Grisafi, P., Fink, G.R., and Bartel, B. (1997). Arabidopsis mutants resistant to the auxin effects of indole-3-acetonitrile are defective in the nitrilase encoded by the NIT1 gene. Plant Cell **9:** 1781–1790.

Nour-Eldin, H.H., Hansen, B.G., Norholm, M.H., Jensen, J.K., and Halkier, B.A. (2006). Advancing uracil-excision based cloning towards an ideal technique for cloning PCR fragments. Nucleic Acids Res. **34:** e122.

Omura, T., and Sato, R. (1964). The carbon monoxide-binding pigment of liver microsomes. II. Solubilization, purification, and properties. J. Biol. Chem. **239:** 2379–2385.

Parisy, V., Poinssot, B., Owsianowski, L., Buchala, A., Glazebrook, J., and Mauch, F. (2007). Identification of PAD2 as a γ-glutamylcysteine synthetase highlights the importance of glutathione in disease resistance of Arabidopsis. Plant J. **49:** 159–172.

Park, W.J., Kriechbaumer, V., Müller, A., Piotrowski, M., Meeley, R.B., Gierl, A., and Glawischnig, E. (2003). The nitrilase ZmNIT2 converts indole-3-acetonitrile to indole-3-acetic acid. Plant Physiol. **133:** 794–802.

Pedras, M.S., Nycholat, C.M., Montaut, S., Xu, Y., and Khan, A.Q. (2002). Chemical defenses of crucifers: Elicitation and metabolism of phytoalexins and indole-3-acetonitrile in brown mustard and turnip. Phytochemistry **59:** 611–625.

Pollmann, S., Müller, A., and Weiler, E.W. (2006). Many roads lead to ''auxin'': Of nitrilases, synthases, and amidases. Plant Biol. (Stuttg.) **8:** 326–333.

Porchia, A.C., Sorensen, S.O., and Scheller, H.V. (2002). Arabinoxylan biosynthesis in wheat. Characterization of arabinosyltransferase activity in Golgi membranes. Plant Physiol. **130:** 432–441.

Rausch, T., Helmlinger, J., and Hilgenberg, W. (1985). High-performance liquid-chromatographic separation and some properties of (E)-3-indoleacetaldoxime and (Z)-3-indoleacetaldoxime. J. Chromatogr. **318:** 95–102.

Reuber, T.L., Plotnikova, J.M., Dewdney, J., Rogers, E.E., Wood, W., and Ausubel, F.M. (1998). Correlation of defense gene induction defects with powdery mildew susceptibility in Arabidopsis enhanced disease susceptibility mutants. Plant J. **16:** 473–485.

Rosso, M.G., Li, Y., Strizhov, N., Reiss, B., Dekker, K., and Weisshaar, B. (2003). An *Arabidopsis thaliana* T-DNA mutagenized population (GABI-Kat) for flanking sequence tag-based reverse genetics. Plant Mol. Biol. **53:** 247–259.

Schenkman, J.B., Remmer, H., and Estabrook, R.W. (1967). Spectral studies of drug interaction with hepatic microsomal cytochrome. Mol. Pharmacol. **3:** 113–123.

Schmidt, R., Müller, A., Hain, R., Bartling, D., and Weiler, E. (1996). Transgenic tobacco plants expressing the *Arabidopsis thaliana* nitrilase II enzyme. Plant J. **9:** 683–691.

Schuhegger, R., Nafisi, M., Mansourova, M., Petersen, B.L., Olsen, C.E., Svatos, A., Halkier, B.A., and Glawischnig, E. (2006). CYP71B15 (PAD3) catalyzes the final step in camalexin biosynthesis. Plant Physiol. **141:** 1248–1254.

Schuler, M.A., and Werck-Reichhart, D. (2003). Functional genomics of P450s. Annu. Rev. Plant Biol. **54:** 629–667.

Sessions, A., et al. (2002). A high-throughput Arabidopsis reverse genetics system. Plant Cell **14:** 2985–2994.

Thomma, B.P., Nelissen, I., Eggermont, K., and Broekaert, W.F. (1999). Deficiency in phytoalexin production causes enhanced susceptibility of *Arabidopsis thaliana* to the fungus *Alternaria brassicicola*. Plant J. **19:** 163–171.

van Wees, S.C., Chang, H.S., Zhu, T., and Glazebrook, J. (2003). Characterization of the early response of Arabidopsis to *Alternaria brassicicola* infection using expression profiling. Plant Physiol. **132:** 606–617.

Voinnet, O., Rivas, S., Mestre, P., and Baulcombe, D. (2003). An enhanced transient expression system in plants based on suppression of gene silencing by the p19 protein of tomato bushy stunt virus. Plant J. **33:** 949–956.

von Malek, B., van der Graaff, E., Schneitz, K., and Keller, B. (2002). The Arabidopsis male-sterile mutant dde2-2 is defective in the ALLENE OXIDE SYNTHASE gene encoding one of the key enzymes of the jasmonic acid biosynthesis pathway. Planta **216:** 187–192.

Vorwerk, S., Biernacki, S., Hillebrand, H., Janzik, I., Müller, A., Weiler, E.W., and Piotrowski, M. (2001). Enzymatic characterization of the recombinant *Arabidopsis thaliana* nitrilase subfamily encoded by the NIT2/NIT1/NIT3-gene cluster. Planta **212:** 508–516.

Wildermuth, M.C., Dewdney, J., Wu, G., and Ausubel, F.M. (2001). Isochorismate synthase is required to synthesize salicylic acid for plant defence. Nature **414:** 562–565.

Zhao, Y., Hull, A.K., Gupta, N.R., Goss, K.A., Alonso, J., Ecker, J.R., Normanly, J., Chory, J., and Celenza, J.L. (2002). Trp-dependent auxin biosynthesis in Arabidopsis: Involvement of cytochrome P450s CYP79B2 and CYP79B3. Genes Dev. **16:** 3100–3112.

Zhou, N., Tootle, T.L., and Glazebrook, J. (1999). Arabidopsis *PAD3*, a gene required for camalexin biosynthesis, encodes a putative cytochrome P450 monooxygenase. Plant Cell **11:** 2419–2428.

Zhou, N., Tootle, T.L., Tsui, F., Klessig, D.F., and Glazebrook, J. (1998). *PAD4* functions upstream from salicylic acid to control defense responses in Arabidopsis. Plant Cell **10:** 1021–1030.

Zimmermann, P., Hirsch-Hoffmann, M., Hennig, L., and Gruissem, W. (2004). GENEVESTIGATOR. Arabidopsis microarray database and analysis toolbox. Plant Physiol. **136:** 2621–2632.

Zook, M., and Hammerschmidt, R. (1997). Origin of the thiazole ring of camalexin, a phytoalexin from *Arabidopsis thaliana*. Plant Physiol. **113:** 463–468.